BMC Cardiovascular Disorders

RESEARCH

Open Access

Blocking $Na_V1.8$ regulates atrial fibrillation inducibility and cardiac conduction after myocardial infarction

Baozhen Qi[1,2†], Zhonglei Xie[1†], Dongli Shen[3†], Yu Song[1], Shaowen Liu[4], Qibing Wang[1*], Jingmin Zhou[1*] and Junbo Ge[1]

Abstract

Background The role of $Na_V1.8$ impacts in atrial fibrillation susceptibility after myocardial infarction remains only partially understood. We studied the effect of blocking $Na_V1.8$ in the cardiac ganglionated plexi (GP) on the atrial fibrillation inducibility and cardiac conduction in the myocardial infarction model.

Methods Eighteen male beagles were randomly enrolled. Left anterior descending coronary artery was ligated to created myocardial infarction model. Four weeks after surgery, $Na_V1.8$ blocker A-803,467 ($n=9$) or DMSO ($n=9$, control) was injected into the four cardiac major GPs. Sinus rate, ventricular rate during atrial fibrillation, PR interval, atrial effective refractory period, atrial fibrillation duration and the cumulative window of atrial vulnerability were measured before and 60 min after A-803,467 injection.

Results Administration of A-803,467 significantly increased sinus rate, shortened PR interval and increased ventricular rate during atrial fibrillation compared to control. A-803,467 also significantly shortened atrial effective refractory period, prolonged atrial fibrillation duration and increased the cumulative window of atrial vulnerability. A-803,467 suppressed the slowing of heart rate response to high-frequency electrical stimulation of the anterior right GP, which was used as the surrogate marker for GP function. Double staining of ChAT and $Na_V1.8$ demonstrated colocalization of ChAT and $Na_V1.8$ in canine GPs.

Conclusions Blocking $Na_V1.8$ in the cardiac GP may modulate atrial fibrillation inducibility and cardiac conduction after myocardial infarction, and the underlying mechanism may be associated with the regulation of the neural activity of the cardiac GP.

Keywords Atrial fibrillation, Cardiac conduction, Ischemia heart disease, Ganglionated plexi, $Na_V1.8$

†Baozhen Qi, Zhonglei Xie and Dongli Shen contributed equally to this work.

*Correspondence:
Qibing Wang
wang.qibing@zs-hospital.sh
Jingmin Zhou
zhou.jingmin@zs-hospital.sh.cn

[1]Department of Cardiology, Zhongshan Hospital, Shanghai Institute of Cardiovascular Disease, National Clinical Research Center for Interventional Medicine, Fudan University, Shanghai 200032, China
[2]Department of Cardiology, Zhongshan Hospital (Xiamen), Fudan University, 668 Jinhu Road, Xiamen 361015, China
[3]Division of Cardiology, Department of Medicine, the Affiliated People's Hospital of Jiangsu University, Zhenjiang 212002, Jiangsu, China
[4]Department of Cardiology, School of Medicine, Shanghai General Hospital, Shanghai Jiao Tong University, Shanghai 200080, China

Background

Atrial fibrillation (AF) is the most frequently occurring supraventricular tachycardia after myocardial infarction (MI) with an incidence between 6 and 21%, which leads to greater risk for heart failure-related hospitalization and mortality [1, 2]. AF first recorded in the first 30 days after MI is independently associated with higher risks of death and ischemic stroke than those in patients with no AF or previously known AF [3]. MI is accompanied by pathological neural remodeling of the autonomic nervous system [4]. The intrinsic cardiac autonomic nervous system is a complex neural network formed by ganglionated plexi (GP) concentrated within epicardial fat pads and the interconnecting nerves, which has been implicated in AF and cardiac conduction [5, 6].

SCN10A encodes the alpha subunit of $Na_V1.8$. $Na_V1.8$ is a tetrodotoxin-resistant sodium channel and mainly expressed in dorsal root ganglia, which is known to play a key role in pain perception [7]. Recently, $Na_V1.8$ has been identified in cardiac GP and cardiac nerve fibers [8–12]. Several genome-wide association studies have shown that *SCN10A*/$Na_V1.8$ is associated with cardiac conduction and AF in the general population and the human failing heart, as well as a lower risk of ventricular fibrillation after MI [12–16]. Although recent studies demonstrated that $Na_V1.8$ contributes to late Na^+ current generation and AF susceptibility [16–19], the presence of $Na_V1.8$ in atrial cardiomyocytes and its contribution to AF is still debated. Transcripts of *SCN10A* were not detected in the left atrial appendage and right atrial appendage form patients with permanent AF [20]. *SCN10A* expression is low in human right atrium tissue, with significantly reduced *SCN10A* levels in chronic AF samples compared to sinus rhythm [21]. Additionally, Casini et al. could not detect any $Na_V1.8$-based peak or late Na^+ current in left atrial appendage-cardiomyocytes from patients with persistent AF [22], consistent with their previous studies in non-diseased human left atrial appendage-cardiomyocytes, human-induced pluripotent stem cell-derived cardiomyocytes, and murine ventricular cardiomyocytes [9, 11]. Our research, along with that of others, has demonstrated that $Na_V1.8$ is specifically expressed in canine, murine and human cardiac neurons [8–10, 15], suggesting a role for the *SCN10A* gene product in cardiac electrophysiology through the modulation of action potential firing in intracardiac neurons [9, 10, 15, 23]. However, the mechanisms by which $Na_V1.8$ influences cardiac electrical function remain only partially understood. Notably, to our knowledge, electrophysiological studies in the MI model aimed at defining association of $Na_V1.8$ and AF susceptibility are limited. To address this issue, our study aimed to investigate the effect of blocking $Na_V1.8$ in the cardiac GP using the blocker A-803,467 on the AF inducibility and cardiac conduction in the MI model.

Materials and methods

Experimental design and surgical protocol

The experimental protocol (Fig. 1a) was approved by Zhongshan Hospital Institutional Animal Care and Use Committee. Experiments were conducted on male beagles weighing 15 to 20 kg. Animals were anaesthetized with an intramuscular injection of ketamine (30 mg/kg) and xylazine (2.2 mg/kg). Once tranquilized, the dogs were intubated, mechanically ventilated, and anesthesia was maintained by 1-2% isoflurane/O_2. Normal saline was infused at 100 ml/h to compensate for spontaneous fluid losses. The dogs were placed on a heating pad to maintain body temperature at 36.5±1 °C. Blood pressure and standard surface ECG were continuously recorded throughout the experiment. All efforts were made to minimize suffering. At the end of the study, the animals were euthanized with a lethal dose of pentobarbital (100 mg/Kg, IV).

Following a median sternotomy, the heart was exposed using a pericardial cradle. The left anterior descending coronary artery (LAD) was permanent ligated with a 3.0 silk suture positioned approximately halfway from the apex to induce MI. Successful ligation was confirmed by the presence of a large homogeneous cyanosis with bulging and ST-segment changes in the surface ECG signal.

Four weeks after surgery, eighteen beagles were randomly assigned to either a control group (n=9) and a A-803,467 group (n=9). A-803,467 (TargetMol, T2024) was dissolved in DMSO. DMSO (0.5mL at each GP, control) or A-803,467 (1μmol/0.5mL at each GP) was injected into four major GPs within four epicardial fat pads (Fig. 1b): (1) superior left GP, located at the left superior pulmonary vein-atrial junction; (2) anterior right GP (ARGP), situated at the right superior pulmonary vein-atrial junction; (3) inferior left GP, located at the left inferior pulmonary vein-atrial junction; and (4) inferior right GP, situated near the junction of the inferior vena cava and both atria. A bipolar electrode probe (AtriCure, West Chester, Ohio, USA) was connected to a Grass S88 stimulator (Grass Technologies, Warwick, RI) for high-frequency electrical stimulation (HFS, 20 Hz, square waves, 0.1ms duration) to localize the cardiac GPs, and progressive slowing of sinus rate or atrioventricular conduction was observed.

Electrophysiological study protocol

The electrophysiological study protocol was applied at baseline and 60 min after drug injection. Multi-electrode catheters (Capsure Epi, Medtronic, Minneapolis, MN, USA) were sutured to the surface of the atrium and pulmonary veins to perform pacing with twice the diastolic pacing threshold. The ECG and intracardiac tracings were recorded and amplified on a Bard Computerized

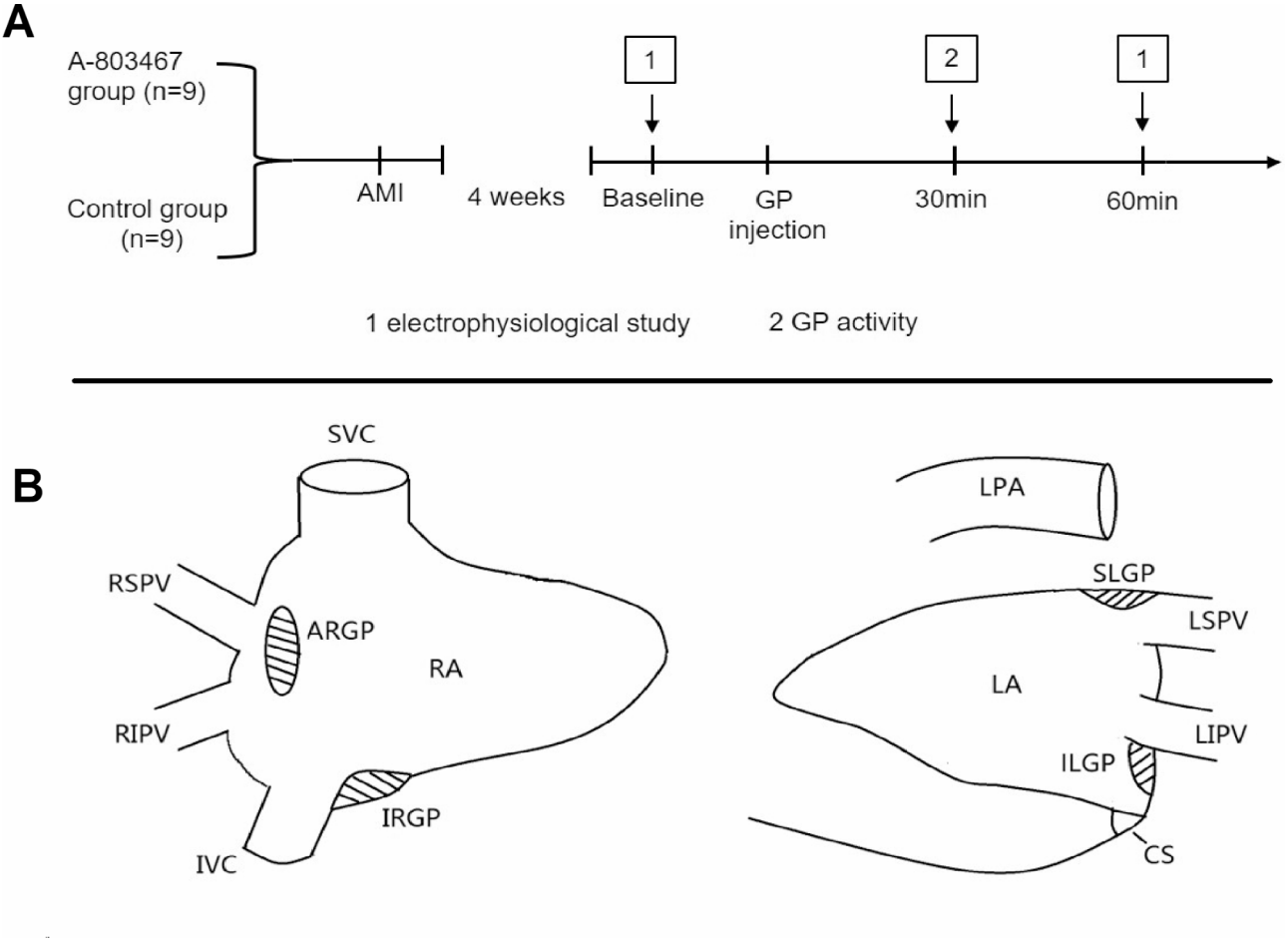

Fig. 1 Schematic representation of the study protocol (**a**) and positions of cardiac ganglionated plexis (**b**). ARGP, anterior right ganglionated plexi; IRGP, inferior right ganglionated plexi; SLGP, superior left ganglionated plexi; ILGP, inferior left ganglionated plexi; SVC, superior vena cava; RSPV, right superior pulmonary vein; RIPV, right inferior pulmonary vein; IVC, inferior vena cava; RA, right atrium; LSPV, left superior pulmonary vein; LIPV, left inferior pulmonary vein; LPA, left pulmonary artery; CS, coronary sinus; LA, left atrium

Electrophysiology system (CR Bard Inc., Bard, Billerica, Massachusetts, USA).

Sinus rate (SR) was calculated using the average R-R interval of 20 beats. PR interval was defined as the interval from the onset of the P-wave to the end of the PR segment. AF was defined as a rapid (>400 bpm) atrial arrhythmia with irregular RR intervals lasting longer than 1 s, which was induced by rapid atrial pacing (20 Hz, 400 impulses) at right and left atrial free walls. The average AF duration was recorded for each group. Ventricular rate (VR) was determined from the ventricular cycle lengths over the last 20 beats during induced AF. Atrial pacing was performed at a cycle length of 300ms (S_1-S_1), and the effective refractory period (ERP) was started at 250ms and repeated with progressively shorter S_1-S_2 intervals until the capture failed (S_1:S_2=8:1). The ERP was defined as the longest S_1-S_2 interval that failed to capture the atria or pulmonary veins. The window of vulnerability (WOV) was defined as the longest S_1-S_2 minus the shortest S_1-S_2 that induced AF. The cumulative window of vulnerability (ΣWOV), defined as the sum of the individual WOVs from right and left atria free walls, was used to measure AF inducibility.

To verify whether the effects of A-803,467 were mediated by modulating GP activity, we examined GP function at 30 min after DMSO or A-803,467 local injection into the ARGP. Voltage-heat rate (HR) response curves were constructed by applying HFS (20 Hz, square waves, 0.1ms duration) to the ARGP with increasing voltages. The change of HR response to ARGP stimulation at each voltage level was used as a surrogate marker for GP function [24].

Immunofluorescence study

Cardiac GPs were fixed in 4% paraformaldehyde for 30 min. Tissue sections were incubated at 4 °C overnight with primary antibody specific for mouse polyclonal anti-Nav1.8 (1:200, ab93616 Abcam, Cambridge, UK), and rabbit polyclonal anti-choline acetyltransferase (ChAT, 1:200, ab181023, Abcam, Cambridge, UK). According

to a different source of primary antibody, Alexa Fluor 488-conjugated secondary antibody was then added and incubated at room temperature for 60 min. A Nikon laser scanning confocal microscope (Eclipse Ni, Nikon, Japan) was used to visualize stained samples.

Statistical analysis

Data are reported as mean±SEM. Repeated measures analysis of variance (ANOVA) was performed to compare the mean of SR, VR, PR interval, ERP, AF duration and ΣWOV between the two groups. Tukey's method was used to adjust for multiple comparisons for all pairwise testing. Repeated measures ANOVA was also performed to compare the slowing of HR with incremental stimulation voltage between groups. GraphPad Prism software version 6.0 (GraphPad Software, La Jolla, California) was used for statistical analysis. Statistical significance was defined as $P<0.05$.

Results

Effect of A-803,467 on SR, PR interval and VR

Injection of A-803,467 into cardiac GPs significantly increased SR compared to the control group after MI ($P<0.05$, $n=9$, Fig. 2A). The PR interval was shortened 60 min after A-803,467 injection; whereas these changes were not significant in the control group ($P<0.05$, $n=9$, Fig. 2B). A-803,467 injection into cardiac GPs significantly increased VR during AF compared to control after MI ($P<0.05$, $n=9$, Fig. 2C). These results indicated that blockade of $Na_V1.8$ in GPs can modulate cardiac conduction in MI hearts.

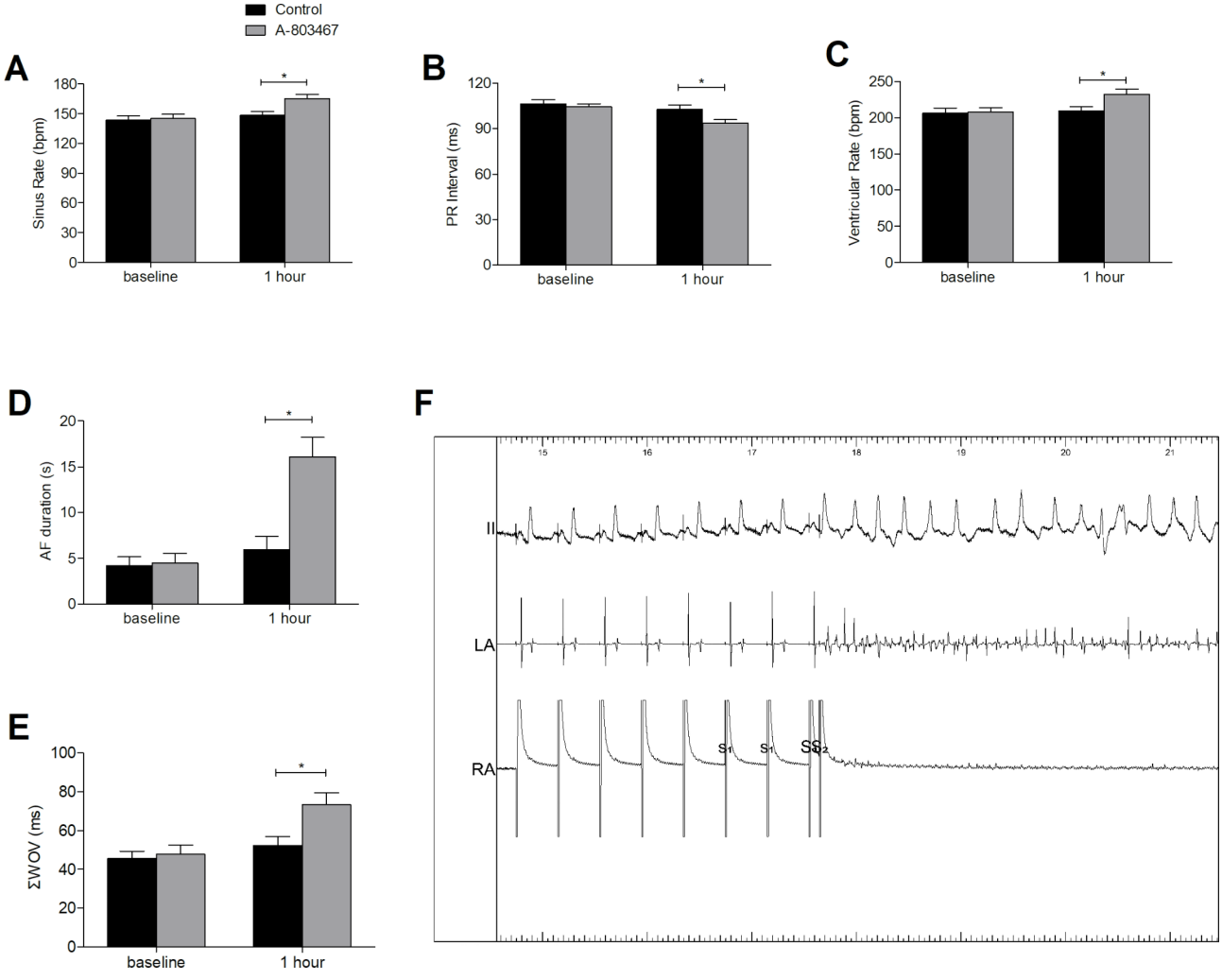

Fig. 2 Effect of A-803,467 on cardiac conduction and atrial fibrillation inducibility in the A-803,467 and control groups. A-803,467 in cardiac GP injection significantly increased sinus rate (**a**), shortened PR interval (**b**) and increased ventricular rate during induced atrial fibrillation (**c**) compared to control after myocardial infarction. (**d**) A-803,467 significantly increased atrial fibrillation duration compared to control. (**e**) A-803,467 significantly increased the ΣWOV compared to control. (**f**) Tracings were lead II of surface ECG, left atrium electrogram and right atrium electrogram. After S1-S2 stimulation applied on the right atrial free wall, atrial fibrillation was initiated. *$P<0.05$ for A-803,467 versus control, $N=9$

Effect of A-803,467 on AF inducibility

The ERPs at all pulmonary vein and atrial sites were significantly shortened 60 min after A-803,467 injection, whereas they remained relatively stable in the control group after MI ($P<0.05$, $n=9$, Fig. 3). Correspondingly, the mean AF duration in the A-803,467 group was longer compared to control ($P<0.05$, $n=9$, Fig. 2D). Additionally, A-803,467 injection into cardiac GPs significantly increased the ΣWOV compared to the control group in MI hearts ($P<0.05$, $n=9$, Fig. 2E and F). The results demonstrated that blocking $Na_V1.8$ in GPs could influence AF inducibility after MI.

Effect of A-803,467 on GP activity

HFS to the ARGP with increasing voltage levels induced a progressive slowing of HR in the control group, while HR remained relatively unchanged after A-803,467 injection. The treatment group by voltage interaction was significant, demonstrating that the trend in the HR change with incremental stimulation voltage is significantly different between the two groups ($P<0.001$, $n=9$, Fig. 4). The result demonstrated that A-803,467 could inhibit the activity of the cardiac GP after MI.

NaV1.8 expression in cardiac GPs

$Na_V1.8$ protein expression was observed in canine GPs through immunohistochemistry staining (Fig. 5). Double staining of ChAT and $Na_V1.8$ not only confirmed the presence of $Na_V1.8$ proteins, but also demonstrated colocalization of ChAT and $Na_V1.8$ in canine GPs.

Discussion

The present study showed that blockade of $Na_V1.8$ increased VR during AF, shortened the PR interval, decreased atrial ERP, and increased the ΣWOV in the MI heart. These effects may be mediated by inhibiting GP activity, as evidenced by the attenuation of the HR response to GP stimulation. The results suggest that blocking $Na_V1.8$ could modulate the AF inducibility and cardiac conduction after MI through the regulation of GP activity.

At first glance, our finding may appear inconsistent with a previous study by our team, which confirmed that blockade of $Na_V1.8$ suppresses the effects of vagus nerve stimulation on PR interval, VR and AF inducibility [23]; However, it is not. Previous studies demonstrated that variants of $Na_V1.8$ are associated with the development of AF and the $Na_V1.8$ selective inhibitor could decrease the incidence of acute AF in structurally normal hearts [10, 25]. The enhancement of sympathetic activity and parasympathetic activity could both frequently increase the onset of AF in patients with structurally normal hearts [26]. Parasympathetic withdrawal and sympathetic overactivity are known to accompany MI, enhancing the risk of atrial arrhythmias [27]. Parasympathetic effects generally counterbalance sympathetic effects and result in beneficial electrophysiological effects following MI [4, 28, 29]. In animal and human studies, MI results in structural and phenotypic changes in GP characteristics, with evidence for sympathetic activation and parasympathetic withdrawal at the level of the GP [4, 30]. The cardiac GP contains both parasympathetic and sympathetic neurons, although most GP neurons have been found to be parasympathetic [31]. Our results suggest that blocking $Na_V1.8$ in the GP could reduce parasympathetic activity, resulting in an imbalance of neural regulation in the heart, thereby promoting the genesis of MI-induced AF (Fig. 6).

Several independent loci of *SCN10A* have been shown to increase PR and/or QRS intervals, suggesting a risk of cardiac conduction abnormalities [32, 33]. Previous studies reported the effects of $Na_V1.8$ on cardiac conduction in structurally normal hearts [12–14]; however, our data suggests that the blockade of $Na_V1.8$ regulates cardiac conduction after MI primarily through the regulating of cardiac GP activity.

To localize the impact on the cardiac GP and reduce its systemic effect on the myocardium, we administered A-803,467 directly into the cardiac GP. We have previously confirmed the presence of *SCN10A*/$Na_V1.8$ in canine GPs but rarely expression in atria and ventricles after acute MI [15]. Multiple investigations have also indicated that $Na_V1.8$ is functionally present in cardiac GP neurons but absent in cardiomyocytes [8–12]. A-803,467 significantly reduced action potential firing frequency in GP neurons without affecting cardiomyocyte resting membrane potential, action potential amplitude, or action potential upstroke velocity [9, 11]. In the present study, A-803,467 reversed the negative chronotropic responses to HFS of the ARGP parasympathetic neural elements, suggesting that blockade of $Na_V1.8$ using A-803,467 could suppress GP activity during MI.

This study used A-803,467 at a dose determined from the literature [34, 35]. After systemic injection, A-803,467 had a 4.9 h plasma elimination half-life and lasted at least 90 min in the SNL model [34]. A-803,467 injection into the neuronal receptive field reduced the evoked discharges of WDR neurons, with the greatest effect observed 35 min after injection [35]. Therefore, we report A-803,467's efficacy in canine GPs for a short period (60 min).

The GP neurons synthesize a variety of neurotransmitters. A previous study found that hyperactive sodium conduction via $Na_V1.8$ leads to marked R-R variability and sinus bradycardia upon pinching the skin at the back of the neck, which could be abrogated by atropine infusion [36]. The loss-of-function of $Na_V1.8$ may decrease the HR in response to atropine, and A-803,467 alleviated

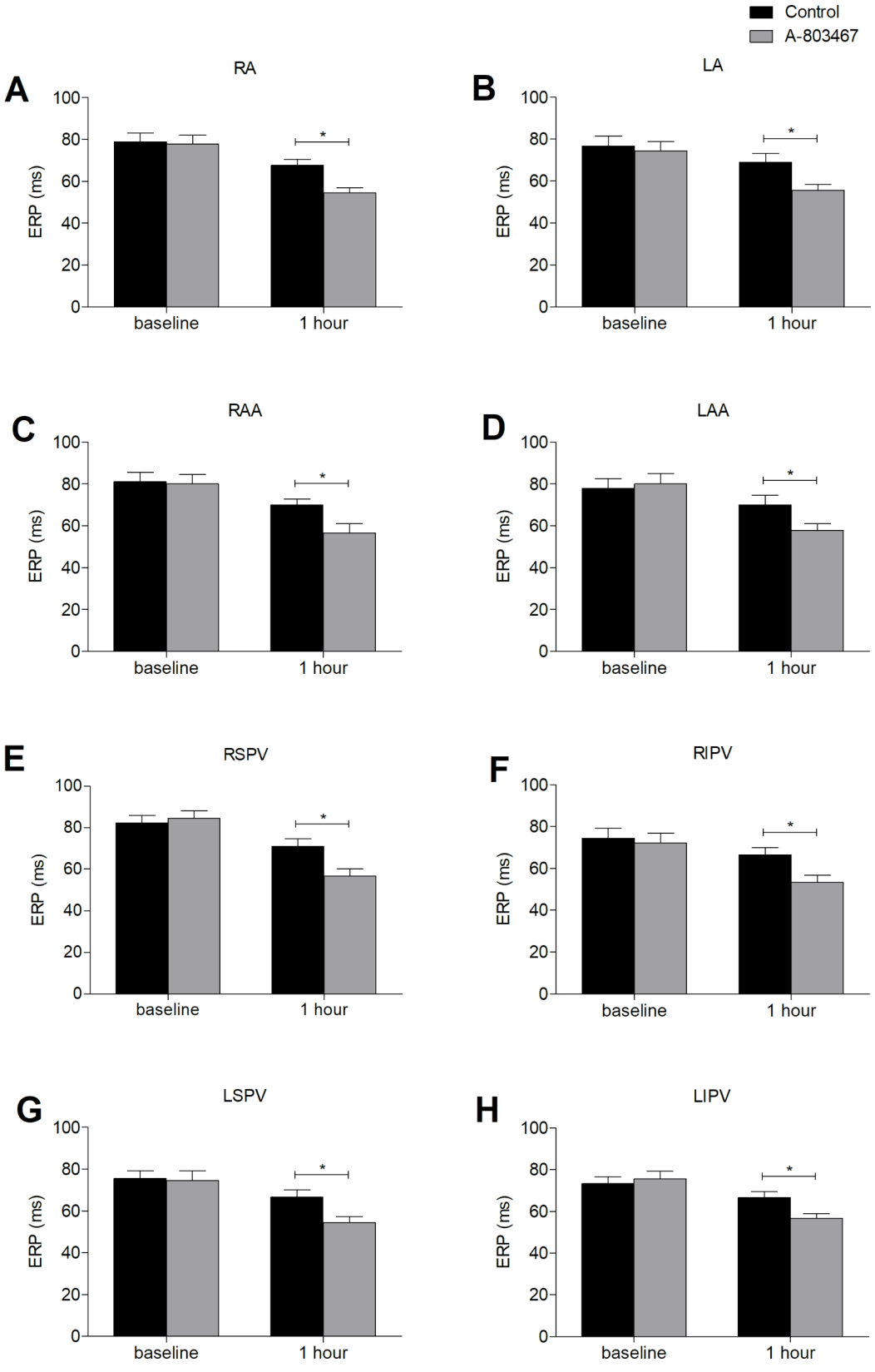

Fig. 3 Effect of A-803,467 on the ERP. At all sites (**a** through **h**), mean ERP was shortened in the A-803,467 group, whereas they remained relatively stable in the control group. * $P < 0.05$ for A-803,467 versus control, $N = 9$. RA, right atrium; LA, left atrium; RAA, right atrial appendage; LAA, left atrial appendage; RSPV, right superior pulmonary vein; RIPV, right inferior pulmonary vein; LSPV, left superior pulmonary vein; LIPV, left inferior pulmonary vein

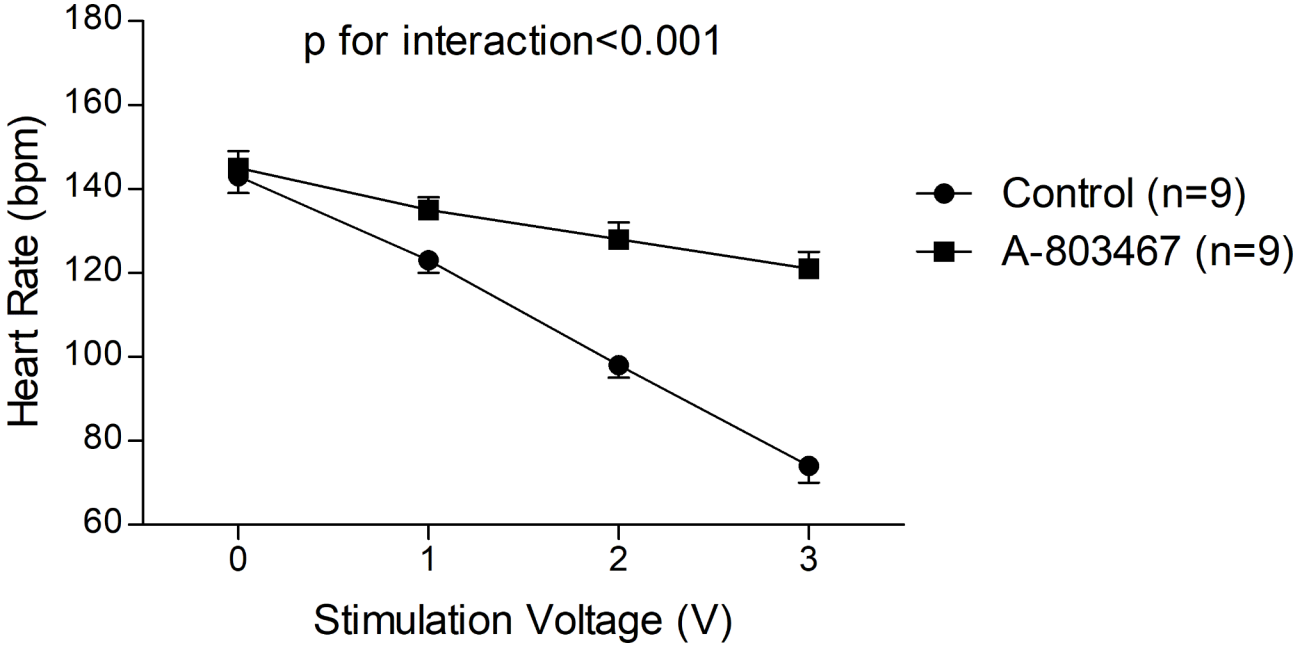

Fig. 4 Effects of A-803,467 on the ganglionated plexi activity at 30 min after injection into the anterior right ganglionated plexi. There was a significantly different trend in the heart rate change with increasing stimulation voltage between the two groups. (*P for interaction* < *0.001*, *N* = 9)

the HR response to atropine in wild-type mice [37]. Brack et al. reported that nitric oxide can play an important role in the anti-fibrillatory effect of vagus nerve stimulation on the rabbit ventricle [38]. We presume that $Na_V1.8$ may influence the release of neurotransmitters in cardiac GPs, with acetylcholine or nitric oxide being potential candidates.

Radiofrequency GP ablation has been demonstrated to improve the short-term success rate of AF ablation; however, it may not achieve long-term effects, and a high AF recurrence rate has been observed after GP ablation alone [39–41]. GP ablation not only significantly decreased the ERP of the atrial and ventricular myocardium but also increased the inducibility of atrial tachyarrhythmia [42]. Additionally, GP ablation increases the risk of ventricular arrhythmias in the MI heart compared to the normal heart, suggesting a protective role of cardiac GP [43]. The present study showed that suppression of GP activity may result in imbalanced modulation of the heart, potentially promoting the genesis of AF after MI.

In contrast to primary AF, where pulmonary vein isolation is effective, there are no established therapies for AF that complicates MI. This is partly due to the current lack of understanding of the mechanisms underlying increased AF susceptibility in this phase. Recent studies may reveal $Na_V1.8$ as a promising antiarrhythmic therapeutic target for clinical AF therapy [16–19]. However, these studies did not attempt to investigate the effect of $Na_V1.8$ in intracardiac neurons, especially in the MI model. Like pharmacological agents that block *SCN5A*, such as flecainide, which were developed as antiarrhythmics, but are proarrhythmic and increase mortality in patients with structural heart disease. Pharmacological inhibition of the $Na_V1.8$ effects should be approached with caution in patients with structural heart disease such as ischemic heart disease.

There are several limitations to our study. Firstly, the anesthesia was maintained with 1-2% isoflurane/O_2, which may have potential influence on GP activity. α-chloralose has been used in many earlier studies and seemed to have little effect on GP activity, but it is not acceptable in many research facilities today. Secondly, we did not record GP activity directly; however, we have provided evidence of altered GP activity that correlate well with GP function based on prior studies [24]. Thirdly, our data did not help to explain the increased incidence of AF following MI. Fourthly, the data in the present study were not sufficient to explain the signaling pathway mediating the protective role of $Na_V1.8$. The exact underlying mechanism requires future studies.

In summary, we have demonstrated that blockade of $Na_V1.8$ channels may modulate AF inducibility and cardiac conduction after MI. The underlying mechanism may be associated with the regulation of the neural activity of the cardiac GP. Pharmacological inhibition of the $Na_V1.8$ effects should be approached with caution after MI.

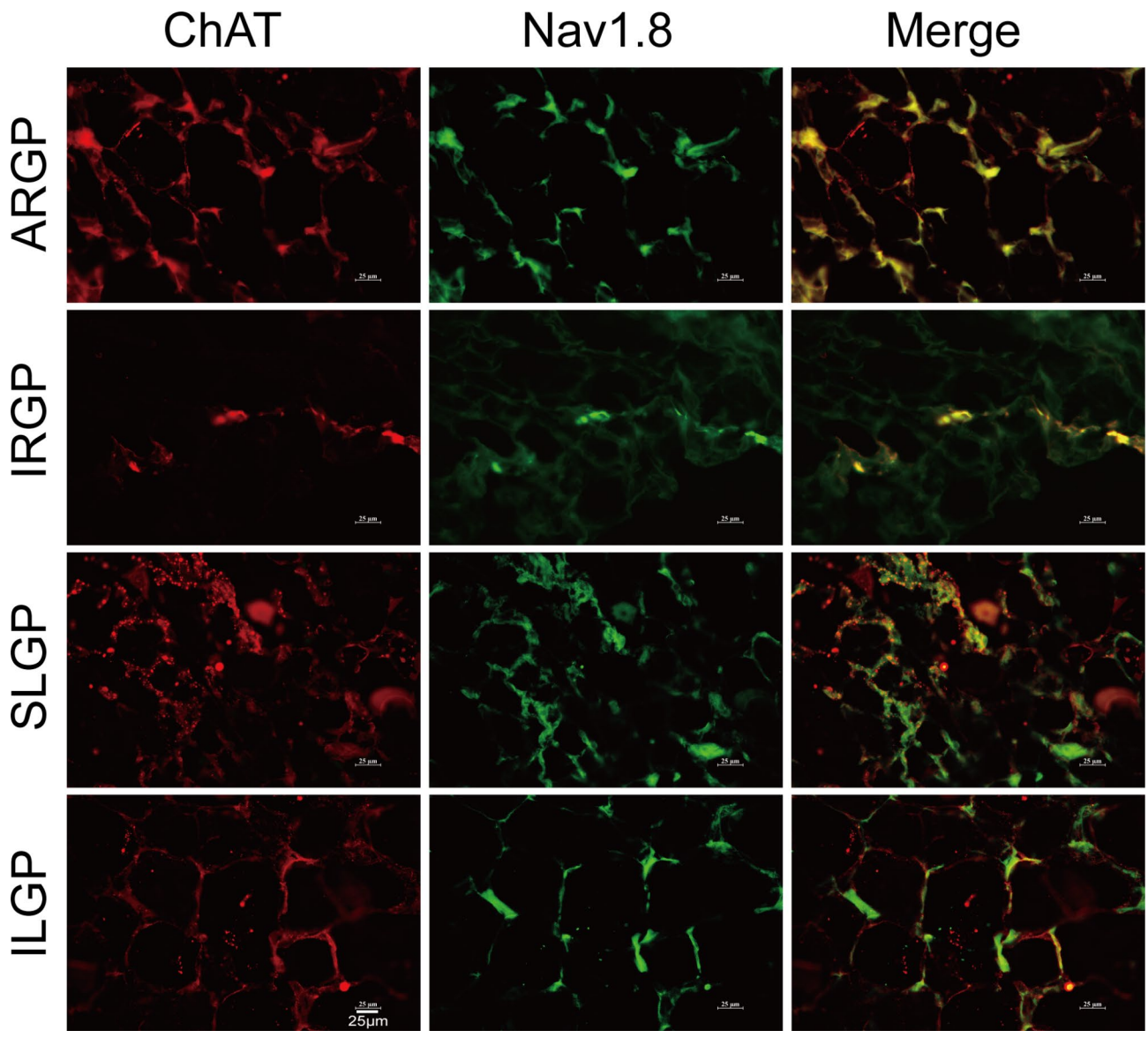

Fig. 5 Examples of ChAT/$Na_V1.8$ double immunofluorescent staining in the cardiac ganglionated plexi after myocardial infarction. The slides show ChAT immunoreactivity (red stain), $Na_V1.8$ immunoreactivity (green stain) and overlapped images of ChAT/$Na_V1.8$ (yellow) immunoreactivity. Calibration bars in the slides are 25 μm. ARGP, anterior right ganglionated plexi; IRGP, inferior right ganglionated plexi; SLGP, superior left ganglionated plexi; ILGP, inferior left ganglionated plexi

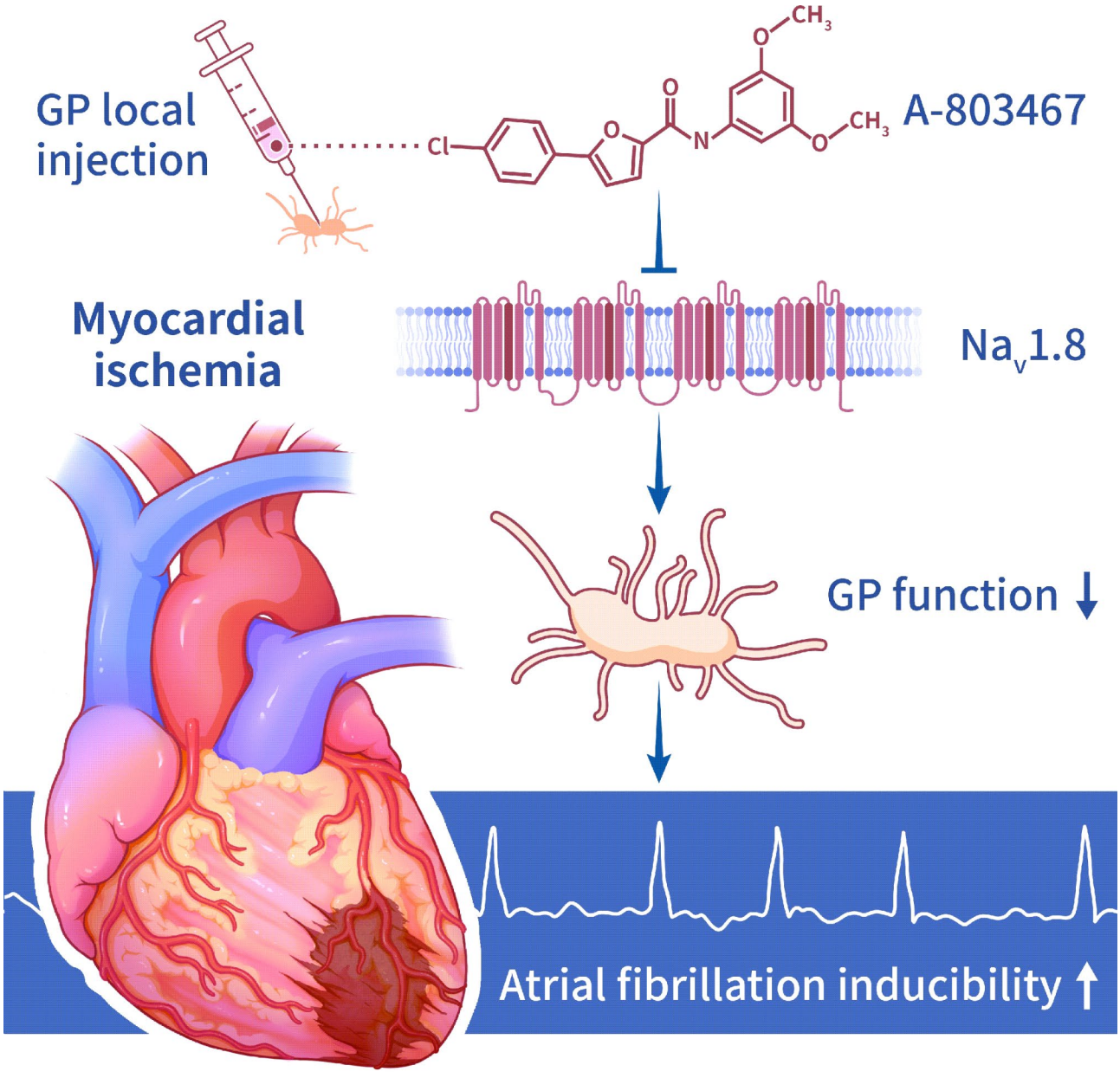

Fig. 6 Schematic diagram depicting the potential role of $Na_V1.8$ channel in atrial fibrillation after myocardial infarction. Parasympathetic effects generally counterbalance sympathetic effects and result in beneficial electrophysiological effects following myocardial infarction. Blocking $Na_V1.8$ in the cardiac ganglionated plexi could reduce parasympathetic activity and may result in an imbalance of neural regulation for the heart, thereby promoting the genesis of ischemia-induced atrial fibrillation

Abbreviations

GP	Ganglionated plexi
AF	Atrial fibrillation
MI	Myocardial infarction
LAD	Left anterior descending coronary artery
ARGP	Anterior right ganglionated plexi
SR	Sinus rate
VR	Ventricular rate
ERP	Effective refractory period
WOV	Window of vulnerability
HR	Heat rate
ChAT	Choline acetyltransferase

Acknowledgements
Not applicable.

Author contributions
BQ performed experiments and wrote the manuscript; ZL and DS performed experiments and collected data; YS and SL performed statistical analysis; QW and JG conceived the idea and designed the study; JZ designed and supervised the study, and revised the manuscript. All authors have read and approved the manuscript.

Funding
This study was supported by the Natural Science Foundation of Shanghai (No. 22ZR1411500), Fujian Provincial Natural Science Foundation of China

(No. 2023J011693) and Shanghai Municipal Key Clinical Specialty (No. shslczdzk01701).

Data availability
The datasets used and analyzed in the current study are available from the corresponding author based on reasonable request.

Declarations

Ethics approval and consent to participate
Animal handling and experimental procedures were approved by Zhongshan Hospital Institutional Animal Care and Use Committee **(No. 2022286)** in accordance with ARRIVE guidelines.

Consent for publication
Not applicable.

Competing interests
The authors declare no competing interests.

Received: 19 October 2023 / Accepted: 14 October 2024
Published online: 29 October 2024

References

1. Schmitt J, Duray G, Gersh BJ, Hohnloser SH. Atrial fibrillation in acute myocardial infarction: a systematic review of the incidence, clinical features and prognostic implications. Eur Heart J. 2009;30:1038–45.
2. Obayashi Y, Shiomi H, Morimoto T, et al. Newly diagnosed Atrial Fibrillation in Acute myocardial infarction. J Am Heart Assoc. 2021;10:e021417.
3. Fauchier L, Bisson A, Bodin A, et al. Outcomes in patients with acute myocardial infarction and new atrial fibrillation: a nationwide analysis. Clin Res Cardiol. 2021;110:1431–8.
4. Vaseghi M, Salavatian S, Rajendran PS, et al. Parasympathetic dysfunction and antiarrhythmic effect of vagal nerve stimulation following myocardial infarction. JCI Insight. 2017;17:2: e86715.
5. Hou Y, Scherlag BJ, Lin J, et al. Ganglionated plexi modulate extrinsic cardiac autonomic nerve input: effects on sinus rate, atrioventricular conduction, refractoriness, and inducibility of atrial fibrillation. J Am Coll Cardiol. 2007;50:61–8.
6. Katritsis DG, Pokushalov E, Romanov A, et al. Autonomic denervation added to pulmonary vein isolation for paroxysmal atrial fibrillation: a randomized clinical trial. J Am Coll Cardiol. 2013;62:2318–25.
7. Abrahamsen B, Zhao J, Asante CO, et al. The cell and molecular basis of mechanical, cold and inflammatory pain. Science. 2008;321:702–5.
8. Facer P, Punjabi PP, Abrari A, et al. Localisation of SCN10A gene product na(v)1.8 and novel painrelated ion channels in human heart. Int Heart J. 2011;52:146–52.
9. Verkerk AO, Remme CA, Schumacher CA, et al. Functional $Na_V1.8$ channels in intracardiac neurons: the link between SCN10A and cardiac Electrophysiology. Circ Res. 2012;111:333–43.
10. Chen X, Yu L, Shi S, et al. Neuronal $Na_V1.8$ channels as a novel therapeutic target of acute atrial fibrillation prevention. J Am Heart Assoc. 2016;5:e004050.
11. Casini S, Marchal GA, Kawasaki M, et al. Absence of functional Nav1.8 channels in non-diseased atrial and ventricular cardiomyocytes. Cardiovasc Drugs Ther. 2019;33:649–60.
12. Man JCK, Bosada FM, Scholman KT, et al. Variant intronic enhancer controls *SCN10A-short* expression and heart conduction. Circulation. 2021;144:229–42.
13. Chambers JC, Zhao J, Terracciano CM, et al. Genetic variation in SCN10A influences cardiac conduction. Nat Genet. 2010;42:149–52.
14. Delaney JT, Muhammad R, Shi Y, et al. Common SCN10A variants modulate PR interval and heart rate response during atrial fibrillation. Europace. 2014;16:485–90.
15. Qi B, Dai S, Song Y, et al. Blockade of $Na_V1.8$ increases the susceptibility to ventricular arrhythmias during Acute myocardial infarction. Fron Cardiovasc Med. 2021;8:708279.
16. Dybkova N, Ahmad S, Pabel S, et al. Differential regulation of sodium channels as a novel proarrhythmic mechanism in the human failing heart. Cardiovasc Res. 2018;114:1728–37.
17. Ahmad S, Tirilomis P, Pabel S, et al. The functional consequences of sodium channel $Na_V1.8$ in human left ventricular hypertrophy. ESC Heart Fail. 2019;6:154–63.
18. Bengel P, Ahmad S, Tirilomis P, et al. Contribution of the neuronal sodium channel $Na_V1.8$ to sodium- and calcium-dependent cellular proarrhythmia. J Mol Cell Cardiol. 2020;144:35–46.
19. Bengel P, Dybkova N, Tirilomis P, et al. Detrimental proarrhythmogenic interaction of Ca^{2+}/calmodulin-dependent protein kinase II and $Na_V1.8$ in heart failure. Nat Commun. 2021;15:12:6586.
20. Hsu J, Hanna P, Van Wagoner DR, et al. Whole genome expression differences in human left and right atria ascertained by RNA sequencing. Circ Cardiovasc Genet. 2012;5:327–35.
21. Poulet C, Wettwer E, Grunnet M, et al. Late sodium current in human atrial cardiomyocytes from patients in sinus rhythm and atrial fibrillation. PLoS ONE. 2015;10:e0131432.
22. Casini S, Marchal GA, Kawasaki M, et al. Differential Sodium current remodelling identifies distinct Cellular Proarrhythmic mechanisms in Paroxysmal vs Persistent Atrial Fibrillation. Can J Cardiol. 2023;39:277–88.
23. Qi B, Wei Y, Chen S, et al. $Na_V1.8$ channels in ganglionated plexi modulate atrial fibrillation inducibility. Cardiovas Res. 2014;102:480–6.
24. Yu L, Scherlag BJ, Li S, et al. Low-level vagosympathetic nerve stimulation inhibits atrial fibrillation inducibility: direct evidence by neural recordings from intrinsic cardiac ganglia. J Cardiovasc Electrophysiol. 2011;22:455–63.
25. Pabel S, Ahmad S, Tirilomis P, et al. Inhibition of $Na_V1.8$ prevents atrial arrhythmogenesis in human and mice. Basic Res Cardiol. 2020;115:20.
26. Capilupi MJ, Kerath SM, Becker LB. Vagus nerve stimulation and the Cardiovascular System. Cold Spring Harb Perspect Med. 2020;10:a034173.
27. Yamaguchi N, Yamakawa K, Rajendran PS, Takamiya T, Vaseghi M. Antiarrhythmic effects of vagal nerve stimulation after cardiac sympathetic denervation in the setting of chronic myocardial infarction. Heart Rhythm. 2018;15:1214–22.
28. Miyauchi Y, Zhou S, Okuyama Y, et al. Altered atrial electrical restitution and heterogeneous sympathetic hyperinnervation in hearts with chronic left ventricular myocardial infarction: implications for atrial fibrillation. Circulation. 2003;22:108:360–6.
29. Tomson TT, Arora R. Modulation of cardiac potassium current by neural tone and ischemia. Card Electrophysiol Clin. 2016;8:349–60.
30. Rajendran PS, Nakamura K, Ajijola OA, et al. Myocardial infarction induces structural and functional remodelling of the intrinsic cardiac nervous system. J Physiol. 2016;594:321–41.
31. Hoover DB, Isaacs ER, Jacques F, Hoard JL, Pagé P, Armour JA. Localization of multiple neurotransmitters in surgically derived specimens of human atrial ganglia. Neuroscience. 2009;164:1170–9.
32. Behr ER, Savio-Galimberti E, Barc J, et al. Role of common and rare variants in SCN10A: results from the Brugada syndrome QRS locus gene discovery collaborative study. Cardiovasc Res. 2015;106:520–9.
33. Fukuyama M, Ohno S, Makiyama T, Horie M. Novel SCN10A variants associated with Brugada syndrome. Europace. 2015;18:905–11.
34. Jarvis MF, Honore P, Shieh CC, et al. A-803467, a potent and selective NaV1.8 sodium channel blocker, attenuates neuropathic and inflammatory pain in the rat. Proc Natl Acad Sci USA. 2007;104:8520–5.
35. McGaraughty S, Chu KL, Scanio MJ, Kort ME, Faltynek CR, Jarvis MF. A selective NaV1.8 sodium channel blocker, A-803467 [5-(4-chlorophenyl-N-(3,5-dimethoxyphenyl)- furan-2-carboxamide], attenuates spinal neuronal activity in neuropathic rats. J Pharmacol Exp Ther. 2008;324:1204–11.
36. Blasiusa AL, Dubinb AE, Petrusc MJ, et al. Hypermorphic mutation of the voltage-gated sodium channel encoding gene Scn10a causes a dramatic stimulus-dependent neurobehavioral phenotype. Proc Natl Acad Sci USA. 2011;108:19413–8.
37. Liu B, Li N, Zhang J, et al. The role of Voltage-gated Sodium Channel 1.8 in the Effect of Atropine on Heart Rate: evidence from a Retrospective Clinical Study and Mouse Model. Front Pharmacol. 2020;11:1163.
38. Brack KE, Patel VH, Coote JH, Ng GA. Nitric oxide mediates the vagal protective effect on ventricular fibrillation via effects on action potential duration restitution in the rabbit heart. J Physiol. 2007;583:695–704.
39. Giannopoulos G, Kossyvakis C, Angelidis C, et al. Coincidental ganglionated plexus modification during radiofrequency pulmonary vein isolation and post-ablation arrhythmia recurrence. Europace. 2017;19:1967–72.
40. Mikhaylov E, Kanidieva A, Sviridova N, et al. Outcome of anatomic ganglionated plexi ablation to treat paroxysmal atrial fibrillation: a 3-year follow-up study. Europace. 2011;13:362–70.

41. Lo LW, Scherlag BJ, Chang HY, Lin YJ, Chen SA, Po SS. Paradoxical long-term proarrhythmic efects after ablating the head station ganglionated plexi of the vagal innervation to the heart. Heart Rhythm. 2013;10:751–7.
42. Mao J, Yin X, Zhang Y, et al. Ablation of epicardial ganglionated plexi increases atrial vulnerability to arrhythmias in dogs. Circ Arrhythm Electrophysiol. 2014;7:711–7.
43. He B, Lu Z, He W, et al. Efects of ganglionated plexi ablation on ventricular electrophysiological properties in normal hearts and after acute myocardial ischemia. Int J Cardiol. 2013;168:86–93.

Publisher's note